Time-Delay System Control Based on an Integration of Active Disturbance Rejection and Modified Twice Optimal Control

XIAOYI WANG, YUQIN ZHOU, ZHIYAO ZHAO^{ID}, WEI WEI, AND WEI LI

Beijing Key Laboratory of Big Data Technology for Food Safety, School of Computer and Information Engineering, Beijing Technology and Business University, Beijing 100048, China

Corresponding author: Zhiyao Zhao (zhaozy@btbu.edu.cn)

ABSTRACT Active disturbance rejection control (ADRC) is a kind of effective tool in dealing with dynamic instability, simultaneous internal and external disturbances, nonlinearity, etc. However, the application of ADRC is limited because the input and output signals of the system are not synchronized due to the existence of time-delay impact in a time-delay system. Modified twice optimal control (MTOC) is a control algorithm proposed for the time-delay system. It can effectively compensate the time-delay impact, synchronize the input and output signals of the system, and provide control conditions for a better application of ADRC to system control. In this paper, a new control algorithm, namely active disturbance rejection modified twice optimal control (ADRMTOC), is proposed based on the suppression capability of ADRC to system total disturbance and the compensation ability of MTOC to time-delay impact. The simulation experiments show that the system under this control method has strong robustness and interference suppression ability, which makes ADRMTOC have certain industrial practical values.

INDEX TERMS Time-delay system, active disturbance rejection control, modified twice optimal control, active disturbance rejection modified twice optimal control, robustness.

NOTATION

$r(t)$	Set value
$u(t)$	Control input
$y(t)$	System output
$d(t)$	External disturbance
a_1', a_0', b	Second-order non-time-delay system parameters
w	System external interference signal
f	Total disturbance of system
x_1, x_2, x_3	State vectors
$\omega(t)$	Time function
z_1, z_2, z_3	ESO outputs
$\beta_{10}, \beta_{20}, \beta_{30}$	ESO parameters
ω_0	Observer bandwidth
ω_c	Controller bandwidth
k_0	Appropriate constant
k_p, k_d	Controller gain
k_c	Gain of the closed-loop system
k_1	Feedback coefficients of system
$\mathbf{k} = [k_2, k_3, \cdots, k_\mu], k_{\mu+1}$	Feedback coefficients of time division model
$\boldsymbol{\alpha} = [\alpha_1, \alpha_2, \cdots, \alpha_\mu]$	Internal feedback coefficient of the $(\mu - 1)$ order state observer
K, K_1	Plant gain
T, T_1	Time constant
L, T_1	Time-delay constant
l	Function of L

The associate editor coordinating the review of this manuscript and approving it for publication was Bing Li.

e^{-Ls}	Infinite dimensional delay factor.
μ	Order of time-sharing model
$\boldsymbol{\beta} = [\beta_1, \beta_2, \cdots, \beta_{\mu+1}]$	Parameters of ITAE optimal transfer function
$F_\mu(s)$	$\mu + 1$ order state feedback equation
$W_{d\mu}(s)$	System open-loop transfer function
$\omega_{0\mu}$	Optimal time scale
$F_{\mu e}(s)$	Infinite-dimensional state observer
$W_{d\mu e}(s)$	Infinite dimensional open loop transfer function
K_F	Structural adjustment factor
$W_{d\mu 1}(s)$	Open loop transfer function expansion of the system based on TOC
$\phi_1(s)$	Closed loop transfer function of TOC
c_1	Damping of TOC
$W_{d\mu 2}(s)$	Open loop transfer function expansion of the system based on MTOC
$\phi_2(s)$	Closed loop transfer function of MTOC
c_2	Damping of MTOC
$E_{dm}\%$	Maximum instantaneous drop value

I. INTRODUCTION

Time-delay system is very common, and the delay itself is inevitable. The existence of infinite dimensional delay factor is one of the major causes of system performance degradation and instability [1], [2]. First of all, the time delay is one of the essential characteristic of a dynamic system, and it cannot be completely eliminated even in the most advanced technology fields. Second, with the development of production demand, the plant become more and more complex, and the accurate mathematical description models of plant become more difficult to obtain. Finally, due to the uncertainty of the model and the time-delay, the control of time-delay systems becomes a hot issue.

In recent decades, the analysis of the stability of time-delay systems has attracted extensive attention from domestic and foreign scholars, and some control algorithms have been proposed, such as Smith predictor control [3]–[8], PID [9]–[14], fuzzy control [15]–[20], network control [21]–[26] and iterative learning control(ILC) [27]–[29] algorithm. Smith predictive control is a pure lag compensation control method. It compensates the system's time delay by estimating the dynamic characteristics of the system, and reduces the system overshoot and improves the system response speed by adjusting the controller parameters [3]–[6]. However, the accuracy of Smith's predictive control depends on the accuracy of the system model. When the model is inaccurate or there is external interference, the control performance of the Smith predictive control is significantly reduced. Therefore, in order to improve the control performance of the device, Smith predictive control is often combined with other control algorithms, such as PID and fuzzy control algorithms

[7], [8]. PID control has the advantages of simple structure, good stability, high reliability and easy operation, and it has been the most widely used control method in the field of industrial process control [7], [8]. In the time-delay system, the gain of the PID controller depends on the characteristic equation of the system, which means that the controller needs to be designed according to the expected performance of the system [9]–[14]. Fuzzy control has the characteristics of not relying on the accurate mathematical description model of the system, which makes it have a strong advantage for the time delay system [15]–[20]. Neural network control can map input and output relationships, with self-learning capabilities and massively parallel processing capabilities. Therefore, in the delay system, the neural network can convert the time-delay system into a non-delay system, thereby reducing the control difficulty [21]–[26]. ILC is an iterative search for the appropriate control input by using the data information from the previous action. It does not rely on the accurate mathematical description model of the system, and can realize the control of nonlinear strongly coupled dynamic systems with high uncertainty with a very simple algorithm. However, whether the plant has the nature of repeated motion determines the control performance of the LIC [27]–[29]. The above algorithms have their own advantages and disadvantages.

In addition to the above algorithms, twice optimal control (TOC) and active disturbance rejection control (ADRC) are also widely used in the field of the time-delay control. TOC is an algorithm that fully compensates for the time-delay factor of the system [30]–[33]. However, the overshoot of the TOC control system is unsatisfied. In actual industrial production, this will affect the operation of the machine and even damage the machine. In order to reduce the overshoot of the system, a structural adjustment factor is introduced in the TOC system, which is called modified twice optimal control (MTOC) [34]. However, the robustness of MTOC is not high. ADRC is not dependent on the mathematical model of the system. ADRC uses the Extended State Observer (ESO) to estimate and compensate for the external disturbances and the internal uncertainty of the system. It has strong anti-interference and robustness, and does not rely on the mathematical model of the system [35]–[42]. However, ADRC has not the characteristics of compensating for the time-delay factor. Therefore, ADRC often combines with other algorithms, such as predictors [42], to improve the control performance of the time-delay system. MTOC and ADRC have a lot of research results in the field of the time-delay system control, but they are not combined. The authors also proposes an algorithm that combines TOC and ADRC in [35]. Although the algorithm improves the performance of the system, the system still exist unsatisfied overshoots and oscillations.

In summary, considering the ability of ADRC to compensate for total interference and the advantages of not relying on the accurate mathematical model of the plant, and the MTOC compensation time-delay factor capability, this manuscript proposes an active disturbance rejection modified twice optimal control algorithm (ADRMTOC). Firstly, the
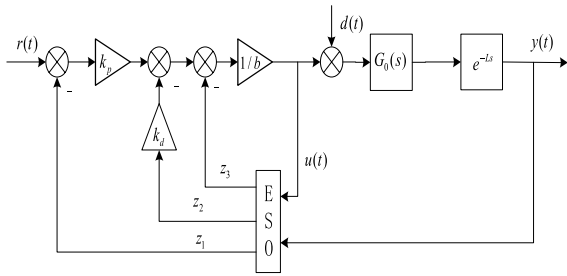
FIGURE 1. Second-order ADRC system.

MTOC controller is used to transform the infinite dimensional delay model of the plant into a finite dimensional non-delay model to achieve compensation control of the time-delay factor of system. Secondly, the plant and the MTOC controller are treated as a generalized plant. Finally, ADRC is used to estimate and compensate the total interference of the generalized system to achieve control of the time delay system.

The rest of the manuscript is organized as follows. First, some preliminaries are introduced in Section 2. The details of the proposed control algorithm are introduced in Section 3, and then some case studies are presented in Section 4. Finally, Section 5 gives conclusions.

II. PRELIMINARIES

This section mainly introduces two types of control algorithms, ADRC and TOC.

A. ADRC

In the case of unknown system mathematical models, ADRC can not only estimate and compensate the external interference signal of the system, but also make a good predictive compensation control for unknown internal disturbances. The core structure of ADRC is the ESO, and the number of parameters of ESO increases as the order of ADRC increases. Therefore, in order to reduce the number of parameters of the ESO, a low-order ADRC is generally used to control the high-order system. The second-order ADRC control structure of the time-delay system is as follows:

where $r(t)$ is the set value, $u(t)$ is the control input, $y(t)$ is the system output, and $d(t)$ is the external disturbance.

In order to better explain the core idea of ADRC, a second-order non-time-delay system is taken as an example, that is, the infinite dimensional delay factor e^{-Ls} is not considered. The mathematical model of the second-order non-time-delay system is:

$$\ddot{y} + a_1'\dot{y} + a_0'y = b(u + w) \tag{1}$$

where $r(t)$ is the set value, $u(t)$ is the control input, $y(t)$ is the system output, and $d(t)$ is the external disturbance.

In the design of ADRC, (1) can be rewritten as:

$$\ddot{y} = bu + f \tag{2}$$

where $f = bw - a_1' - a_0'y$ is the total disturbance of system.

The state equation of the second - order non-time-delay systems is as follows:

$$\begin{cases} \dot{x}_1 = x_2 \\ \dot{x}_2 = f(x_1, x_2, w) + bu \\ y = x_1 \end{cases} \tag{3}$$

To linearize the equation (3), let $x_3 = f(x_1, x_2, w)$, $\dot{x}_3 = \omega(t)$, and $\omega(t)$ is the time function. Then, a second order linearized state equation is obtained:

$$\begin{cases} \dot{x}_1 = x_2 \\ \dot{x}_2 = x_3 + bu \\ \dot{x}_3 = \omega(t) \\ y = x_1 \end{cases} \tag{4}$$

ESO is set up for this expanded system as follows:

$$\begin{cases} \dot{z}_1 = z_2 + \beta_{10}(y - z_1) \\ \dot{z}_2 = z_3 + \beta_{20}(y - z_1) + bu \\ \dot{z}_3 = \beta_{30}(y - z_1) \end{cases} \tag{5}$$

where z_1, z_2 and z_3 are the ESO outputs, β_{10}, β_{20} and β_{30} are the ESO parameters:

$$\begin{cases} \beta_{10} = 3\omega_0 \\ \beta_{20} = 3\omega_0^2 \\ \beta_{30} = \omega_0^2 \\ \omega_0 = k_0\omega_c \end{cases} \tag{6}$$

where ω_0 is the observer bandwidth, ω_c is the controller bandwidth, and k_0 is the appropriate constant.

The control law can be designed as:

$$\begin{cases} u = \dfrac{u_0 - z_3}{b} \\ u_o = k_p(r - z_1) - k_d z_2 \end{cases} \tag{7}$$

where $k_p = \omega_c^2$ and $k_d = 2\omega_c$ are the controller gains.

In summary, the ADRC design process does not consider the infinite dimensional delay factor e^{-Ls}, which means that it can only achieve effective control of the hourly time-delay system. However, the control effect will become unstable or even worse when the system has a large time-delay factor.

B. TOC

TOC is a special algorithm for time-delay system which can effectively compensate the system's time-delay factor. It is mainly divided into two steps: (1) the infinite dimensional delay factor is approximated by the finite dimensional delay factor, and the integral observer and the absolute error (ITAE) optimal control law are used to determine the parameters of the state observer. In this process, ITAE optimization is implemented in a finite dimensional space, which is also the first optimization of TOC. (2) the finite dimensional delay factor is returned to the infinite dimensional delay factor, that is, the delay parameter is returned, and update the parameters of the state observer. In this process, the optimal time scale can be estimated by computer simulation to satisfy
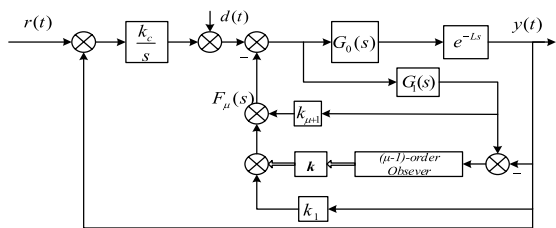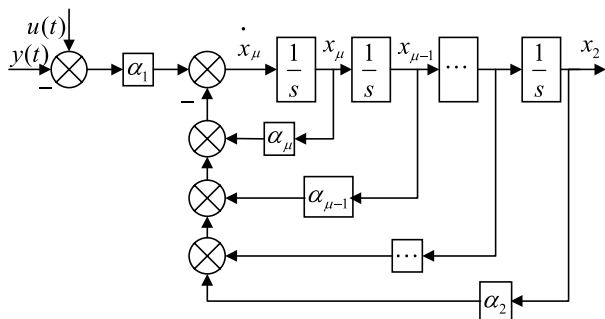
FIGURE 2. System of TOC.

FIGURE 3. Structure of the $(\mu - 1)$-order state observer.

the optimal control rate of ITAE which is also the second optimization of TOC. Its structure is as follows:

In FIGURE 2, k_c is the gain of the closed-loop system; $G_1(s)$ is the prediction transfer function; k_1 is feedback coefficients of system; $\boldsymbol{k} = [k_2, k_3, \cdots, k_\mu]$ and $k_{\mu+1}$ are feedback coefficients of time division models; the $(\mu - 1)$-order state observer structure shown in Figure 3.

In FIGURE 3, $\boldsymbol{\alpha} = [\alpha_1, \alpha_2, \cdots, \alpha_\mu]$ is the internal feedback coefficient of the $(\mu - 1)$ order state observer:

$$\alpha_1 = \frac{\mu!}{L^\mu}, \alpha_2 = \frac{\mu!}{L^{\mu-1}}, \cdots$$
$$\alpha_i = \frac{\mu!}{(i-1)!}\frac{1}{L^{\mu-(i-1)}} \cdots \alpha_\mu = \frac{\mu}{L} \quad (8)$$

Most time-delay systems can be approximated as a first order plus time-delay (FOPTD) model:

$$G(s) = G_0(s)e^{-Ls} = \frac{K}{Ts+1}e^{-Ls} \quad (9)$$

In equation (9), the infinite dimensional delay factor e^{-Ls} is:

$$e^{-Ls} = 1/(\sum_{i=0}^{\infty} l_i s^i), l_i = \frac{1}{i!}L^i \quad i \in N \quad (10)$$

Any physical system is a dissipative system. As time goes on, the dissipation will eliminate all small-scale and faster convergence dimensions in the system. This means that the dimension that determines the long-term behavior of the system will be reduced to a valid number of dimensions. Therefore, the finite dimensional delay factor is used to instead of the infinite dimensional delay factor (10) in TOC:

$$e^{-Ls} = \frac{1}{\sum_{i=0}^{\mu} l_i s^i}, l_i = \frac{1}{i!}L^i \quad \mu \in N \quad (11)$$

where (11) is named as the μ-order time-sharing model, and its corresponding general formula of the $\mu + 1$-order state feedback equation is:

$$F_\mu(s) = \sum_{i=1}^{\mu} k_i s^{i-1} + k_{\mu+1} \sum_{i=0}^{\mu} l_i s^i \quad (12)$$

The system open-loop transfer function is:

$$W_{d\mu}(s) = \frac{k_c G_\mu(s)}{s[1 + G_\mu(s)F_\mu(s)]} \quad (13)$$

where $G_\mu(s) = \frac{K}{Ts+1} \cdot \frac{1}{\sum_{i=0}^{\mu} l_i s^i}$.

Expand $W_{d\mu}(s)$ and compare it with the standard ITAE open-loop transfer function to get the first optimization controller parameter set $\{k_c, k_1, \boldsymbol{k}, k_{\mu+1}\}$ and the parameters of ITAE optimal transfer function $\boldsymbol{\beta} = [\beta_1, \beta_2, \cdots, \beta_{\mu+1}]$, which is as follows:

$$\begin{cases} k_c = \frac{1}{K}TL_\mu\omega_{0\mu}^{\mu+2} \\ k_{\mu+1} = \frac{1}{K}(T\beta_{\mu+1}\omega_{0\mu} - \frac{l_{\mu-1}}{l_\mu}T - 1) \\ k_i = \frac{1}{K}[l_\mu\beta_i T\omega_{0\mu}^{\mu+2-i} - l_{i-1}(Kk_{\mu+1}+1) - l_{i-2}T] \end{cases} \quad (14)$$

where $\omega_{0\mu}$ is the optimal time scale.

In order to achieve the second optimal control, we need to rethink the infinite dimensional delay factor e^{-Ls}, which means that we should return the finite dimensional delay factor (11) to the infinite dimensional delay factor (10). Therefore, the infinite-dimensional state observer is:

$$F_{\mu e}(s) = k_{\mu+1}e^{Ls} + \frac{\sum_{i=0}^{\mu} k_i s^{i-2}}{\sum_{i=1}^{\mu} l_i s^{i-1}}(e^{Ls}-1) + k_1 \quad (15)$$

There is a leading term in equation (15), which makes it a leading infinite dimensional feedback equation. Therefore, it can predict the trend of the output signal, and has the same function as the Smith predictor to compensate for time delay. The corresponding infinite dimensional open loop transfer function is:

$$W_{d\mu e}(s) = \frac{k_c G(s)}{s[1 + G(s)F_{\mu e}(s)]} \quad (16)$$

Equation (16) is a transfer function with both the lead and lag term, which means that it is difficult to find the optimal $\omega_{0\mu}$ by analytical method, but it can be estimated by computer simulation to satisfy the optimal control rate of ITAE. Then, substituting $\omega_{0\mu}$ into equation (14), we can find all the parameters of the twice optimal controller.

In order to better explain the idea of TOC, a 4th order time division model is taken as an example. When $\mu = 4$, the time-sharing model is shown below:

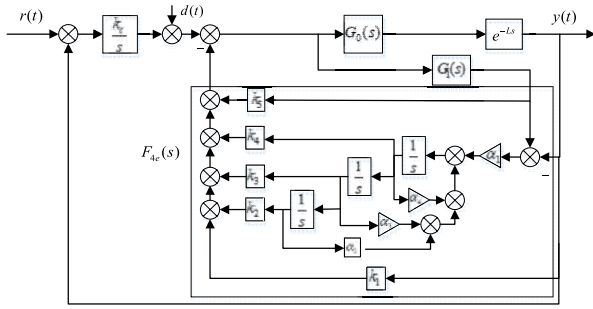$$e^{-Ls} = \frac{1}{1 + Ls + \frac{1}{2}L^2 s^2 + \frac{1}{6}L^3 s^3 + \frac{1}{24}L^4 s^4} \quad (17)$$

FIGURE 4. System diagram of the 4th order time division model.

FIGURE 5. System of MTOC.

The 5-order state feedback equation is:

$$F_4(s) = k_1 + k_2 s + k_3 s^2 + k_4 s^3 + k_5 \sum_{i=0}^{4} l_i s^i \quad (18)$$

The system open-loop transfer function is:

$$W_{d4}(s) = \frac{k_c G_4(s)}{s[1 + G_4(s)F_4(s)]} \quad (19)$$

The first optimization controller parameter set is:

$$\begin{cases} k_c = \dfrac{TL^4 \omega_0^6}{24K} \\ k_1 = \dfrac{\beta_1 TL^4 \omega_0^4}{24K} - \dfrac{\beta_5 T \omega_0}{K} + \dfrac{4T}{KL} \\ k_2 = \dfrac{\beta_2 TL^4 \omega_0^4}{24K} - \dfrac{\beta_5 TL \omega_0}{K} + \dfrac{3T}{K} \\ k_3 = \dfrac{\beta_3 TL^4 \omega_0^3}{24K} - \dfrac{\beta_5 TL^2 \omega_0}{2K} + \dfrac{TL}{K} \\ k_4 = \dfrac{\beta_4 TL^4 \omega_0^2}{24K} - \dfrac{\beta_5 TL^3 \omega_0}{6K} + \dfrac{TL^2}{6K} \\ k_5 = \dfrac{\beta_5 TL^4 \omega_0}{K} - \dfrac{1}{K} - \dfrac{4T}{KL} \end{cases} \quad (20)$$

The infinite dimensional state observer equation is:

$$F_{4e}(s) = k_5 e^{Ls} + \frac{(k_2 + k_3 s + k_4 s^2)\frac{24}{L^4}(e^{Ls}-1)}{s[s(s+\frac{4}{L})+\frac{12}{L^2}+\frac{24}{L^3}]} + k_1 \quad (21)$$

The corresponding infinite dimensional open loop transfer function is:

$$W_{d4e}(s) = \frac{k_c G(s)}{s[1 + G(s)F_{4e}(s)]} \quad (22)$$

In summary, the system diagram of the 4th order time division model as follow:

III. ALGORITHM OF ADRMTOC
In this section, based on the TOC algorithm, the MTOC algorithm is constructed. Then combined with ADRC algorithm to construct ADRMTOC algorithm.
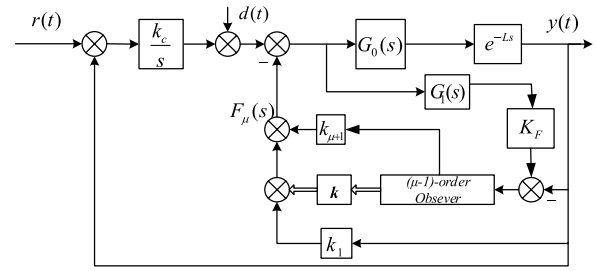
A. MTOC
In order to reduce system shock and improve system stability, the damping of the low frequency band of the system should be increased. Thus, a structural adjustment factor K_F ($K_F > 1$) is introduced in TOC to turn the system into the MTOC. Its structure is as follows:

Form FIGURE 5, the $\mu + 1$-order state feedback equation is changed from equation (12) to the following equation:

$$F_\mu(s) = K_F k_{\mu+1} \sum_{i=0}^{\mu} l_i s^i + K_F \sum_{i=2}^{\mu} k_i s^{i-1} + k_1 \quad (23)$$

Damping analysis of TOC:

1) Put (12) into (13) and the open loop transfer function expansion of the system is:

$$W_{d\mu1}(s) = \frac{k_c K}{A} \quad (24)$$

where:

$$A = s[Tl_\mu s^{\mu+1} + (Tl_{\mu-1} + l_\mu + Kk_{\mu+1}l_\mu)s^\mu + \cdots \\ + (T + l_1 + Kk_2 + Kk_{u+1}l_1)s + (1 + Kk_1 + Kk_{\mu+1})] \quad (25)$$

2) The closed loop transfer function is:

$$\phi_1(s) = \frac{W_{d\mu1}(s)}{1 + W_{d\mu1}(s)} = \frac{k_c K}{Tl_\mu B} \quad (26)$$

where:

$$B = s^{\mu+2} + \frac{Tl_{\mu-1} + l_\mu + Kk_{\mu+1}l_\mu}{Tl_\mu} s^{\mu+1} + \cdots \\ + \frac{T + l_1 + Kk_2 + Kk_{u+1}l_1}{Tl_\mu} s^2 \\ + \frac{1 + Kk_1 + Kk_{\mu+1}}{Tl_\mu} s + \frac{k_c K}{Tl_\mu} \quad (27)$$

3) Let:

$$c_1 = \frac{Tl_{\mu-1} + l_\mu + Kk_{\mu+1}l_\mu}{Tl_\mu} \quad (28)$$

The damping of TOC is closely related to the size of c_1. The larger the c_1 is, the greater the damping is, and vice versa.

Damping analysis of MTOC:

1) Put (23) into (13) and the open loop transfer function expansion of the system is:

$$W_{d\mu2}(s) = \frac{k_cK}{C} \quad (29)$$

where:

$$C = s[Tl_\mu s^{\mu+1} + (Tl_{\mu-1} + l_\mu + Kk_{\mu+1}l_\mu)s^\mu + \cdots \\ + (T + l_1 + Kk_2 + Kk_{u+1}l_1)s + (1 + Kk_1 + Kk_{\mu+1})] \quad (30)$$

2) The closed loop transfer function is:

$$\phi_2(s) = \frac{W_{d\mu2}(s)}{1 + W_{d\mu2}(s)} = \frac{k_cK}{Tl_\mu D} \quad (31)$$

where:

$$D = s^{\mu+2} + \frac{Tl_{\mu-1} + l_\mu + KK_Fk_{\mu+1}l_\mu}{Tl_\mu}s^{\mu+1} + L \\ + \frac{T + l_1 + Kk_2 + Kk_{u+1}l_1}{Tl_\mu}s^2 \\ + \frac{1 + Kk_1 + KK_Fk_{\mu+1}}{Tl_\mu}s + \frac{k_cK}{Tl_\mu} \quad (32)$$

3) Let:

$$c_2 = \frac{Tl_{\mu-1} + l_\mu + KK_Fk_{\mu+1}l_\mu}{Tl_\mu} \quad (33)$$

The damping of MTOC is closely related to the size of c_2. The larger the c_2 is, the greater the damping is, and vice versa.

It can be seen from equations (28) and (33) that $c_1 < c_2$; therefore, the damping of the TOC system is smaller than that of the MTOC system. The introduction of the structural adjustment factor K_F increases the damping of the system, which improves the robustness of the system. At the same time, the response speed of the system will also decrease. In this regard, the system's response speed is often increased by adjusting the gain of the system.

B. ADRMTOC

In summary, considering the ability of ADRC to compensate for total interference and the advantages of not relying on the accurate mathematical model of the plant, and the MTOC compensation time-delay factor capability, this manuscript proposes an active disturbance rejection modified twice optimal control algorithm (ADRMTOC). Firstly, the MTOC controller is used to transform the infinite dimensional delay model of the plant into a finite dimensional non-delay model to achieve compensation control of the time-delay factor of system. Secondly, the plant and the MTOC controller are treated as a generalized plant. Finally, ADRC is used to estimate and compensate the total interference of the generalized system to achieve control of the time delay system. The specific block diagram is shown in FIGURE 6, and the process of the ADRMTOC algorithm are shown in TABLE 1.
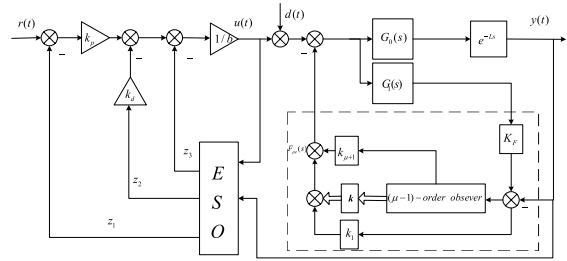

FIGURE 6. System diagram of ADRMTOC.

TABLE 1. The process of the ADRMTOC algorithm.

Step	Content
1	Determining the plant $G(s)$;
2	Design MTOC controller:
	2.1 Set the order of time-sharing model μ ;
	2.2 Set MTOC controller parameters: β 、 $\omega_{0\mu}$ and K_F ;
	2.3 Calculate the parameters $k_c, k_1, \boldsymbol{k}, k_{\mu+1}$ using equation (23) and equations (13)-(16);
3	Treat MTOC and plant as a generalized plant $G_g(s)$;
4	Design ADRC controller:
	4.1 Set the controller to second-order ADRC;
	4.2 Set ADRC controller parameters: b , ω_c and ω_o ;

IV. CASE STUDIES

In order to demonstrate the effectiveness of ADRMTOC, this manuscript selects the first-order plus dead-time plant dead-time plant (FOPDT) as the plant, and uses Smith predictive proportional integral control (SPPI) and predictive active disturbance rejection control (PADRC) algorithm as the comparison algorithm. At the same time, the maximum deviation, the adjustment time, the value of ITAE and the maximum instantaneous drop value $E_{dm}\%$ are selected as evaluation indicators, and the control performance of the algorithm is analyzed from the rapidity and robustness.

A. STABILITY AND ROBUSTNESS TEST

Determining the plant, which is derived from [39]:

$$G(s) = G_0(s)e^{-Ls} = \frac{K}{Ts+1}e^{-Ls} = \frac{0.85}{1200s+1}e^{-1800s} \quad (34)$$

ADRMTOC uses a 4-order time-division model, and some parameters are from [33]:

$$\beta_1 = 4.227, \beta_2 = 8.202, \beta_3 = 9.463, \beta_4 = 7.127, \\ \beta_5 = 3.316, \omega_{0\mu} = \frac{1.999}{L}, K_F = 40 \quad (35)$$

Under ideal conditions, the prediction transfer function is exactly the same as the actual function:

$$G'(s) = G_1(s)e^{-L_1s} = \frac{K_1}{T_1s+1}e^{-L_1s} = \frac{0.85}{1200s+1}e^{-1800s} \quad (36)$$

At the same time, in order to verify the stability and robustness of the time-delay system under the control of

TABLE 2. The parameters under ideal conditions.

Controller	Parameter		
ADRMTOC	b	ω_c	ω_o
	300	1.56	$6\omega_c$
PADRC	b	ω_c	ω_o
	0.0014	0.01	$3\omega_c$
SPPI	k_p	k_i	k_d
	2.28	0.001	0

ADRMTOC, SPPI and ADRC are used as comparison algorithms. The parameter settings are shown in TABLE 2.

The robustness of the system is tested by applying the disturbance signal at 22500 seconds, and the disturbance signal value is twice than the given input value. Under ideal conditions, the experimental results of ADRMTOC, SPPI and PADRC are shown in FIGURE 7. Among them, FIGURE 7(a) is the output response and control input of the system, FIGURE 7(b) is the error response of the system and ITAE; at the same time, the red line is the system set value curve,

the blue line is the result curve of ADRMTOC, the black line is the result curve of SPPI, and the powder line is the result curve of PADRC. The performance index values are shown in TABLE 3.

It can be seen from FIGURE 7 and TABLE 3 that under ideal conditions, the response speed and stability of the system under the control of PADRC and SPPI are faster than that under the control of ADRMTOC. However, when the system receives external disturbances, the robustness of the system under ADRMTOC is much better than that under PADRC and SPPI. Moreover, the ITAE value of ADRMTOC is much smaller than that of PADRC and SPPI.

However, in the actual industrial system, since the system is a dynamic environment, and the system is affected by various factors such as wear of the machine itself, it is impossible to accurately obtain the parameters of the actual model. When the prediction transfer function is as follows:

$$G'(s) = G_1(s)e^{-L_1s} = \frac{K_1}{T_1s + 1}e^{-L_1s} = \frac{1}{1500s + 1}e^{-2000s} \quad (37)$$
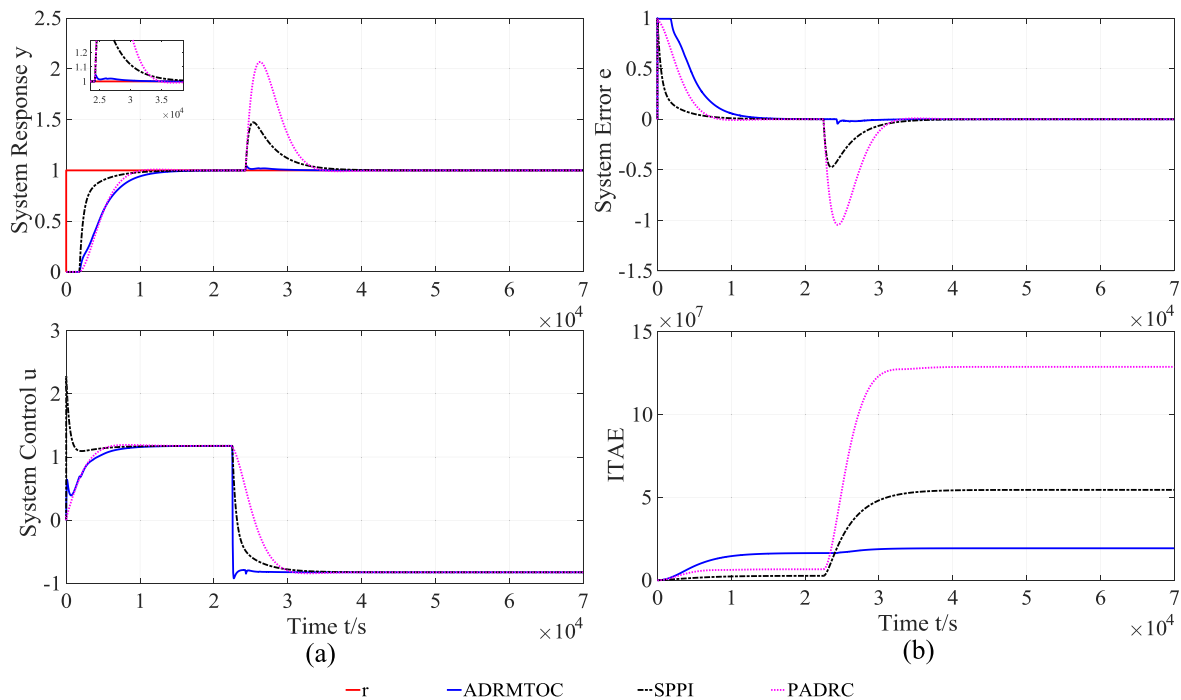

FIGURE 7. Experimental results of ADRMTOC, SPPI and PADRC under ideal conditions.

TABLE 3. Performance indexes under ideal conditions.

Performance index	Controller	SPPI	PADRC	ADRMTOC
Rapidity	Maximum deviation	0	0.01	0
	Adjustment time ($\times 10^4$)	1.0408	1.0408	1.0408
	The value of ITAE ($\times 10^7$)	0.2656	0.6612	1.6413
Robustness	$E_{dm}\%$	0.4737	1.068	0.045
	Adjustment time ($\times 10^4$)	0.1	0.15	0
	The value of ITAE ($\times 10^7$)	5.4546	12.883	1.9283

TABLE 4. Parameters under non-ideal conditions.

Controller		Parameter	
ADRMTOC	b	ω_c	ω_o
	290	2.11	4.1 ω_c
PADRC	b	ω_c	ω_o
	0.0014	0.0012	3ω_c
SPPI	k_p	k_i	k_d
	2.28	0.001	0

The parameter settings are shown in TABLE 4.

Under non-ideal conditions, the experimental results of ADRMTOC, SPPI and PADRC are shown in FIGURE 8. Among them, FIGURE 8(a) is the output response and control input of the system, FIGURE 8(b) is the error response of the system and ITAE; at the same time, the red line is the system set value curve, the blue line is the result curve of ADRMTOC, the black line is the result curve of SPPI, and the

powder line is the result curve of PADRC. The performance index values are shown in TABLE 5.

It can be seen from FIGURE 8 and TABLE 5 that under non-ideal conditions, the stability of time-delay system under the control of ADRMTOC is better than that of SPPI and ADRC. At the same time, the robustness of the system under the control of ADRMTOC is much better than that under the control of PADRC and SPPI, since the ADRMTOC algorithm compensates the delay factor of the system completely, synchronizes the input and output signals of the system, and enables the system to timely suppress the external disturbance information. In addition, the system has the smallest ITAE under the control of ADRMTOC.

In order to better verify the effectiveness of ADRM-TOC on time-delay systems, the parameters of the system are randomly selected in $\Delta K = \pm 40\%$, $\Delta T = \pm 30\%$, $\Delta L = \pm 15\%$ and six groups of parameters are randomly generated by computer simulation for experiments. The experimental results are shown in FIGURE 9. Among them,
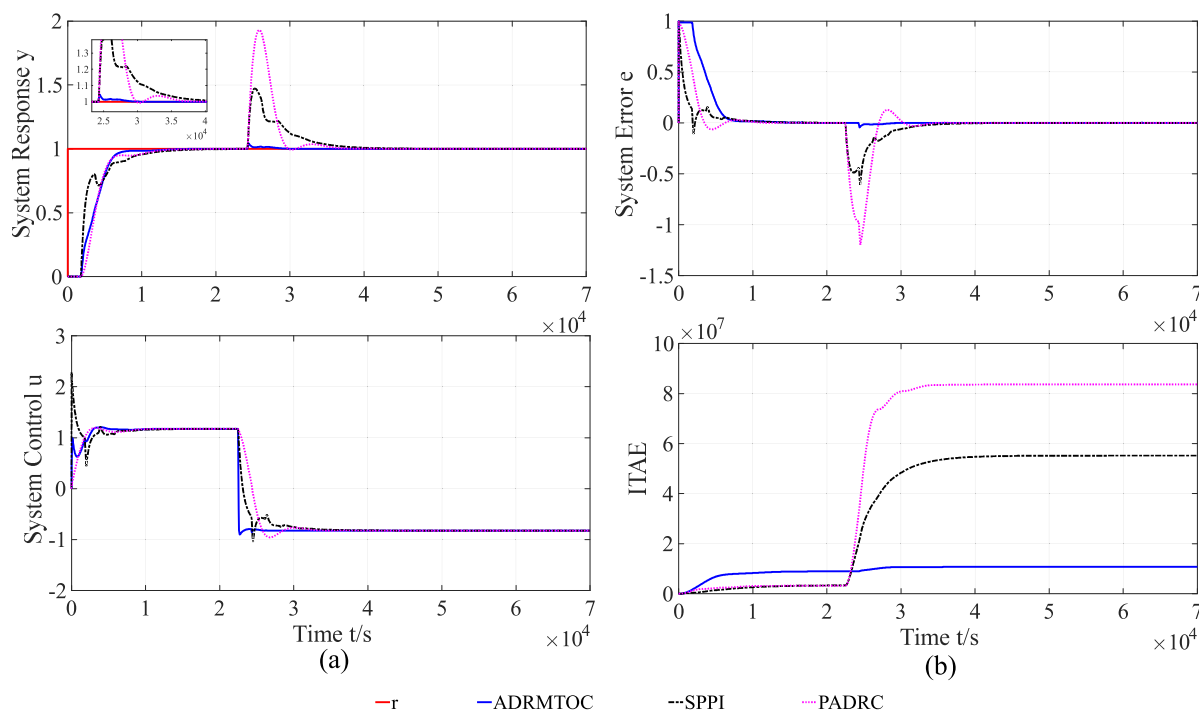

FIGURE 8. Experimental results of A DRMTOC, SPPI and PADRC under non-ideal conditions.

TABLE 5. Performance indexes under non-ideal conditions.

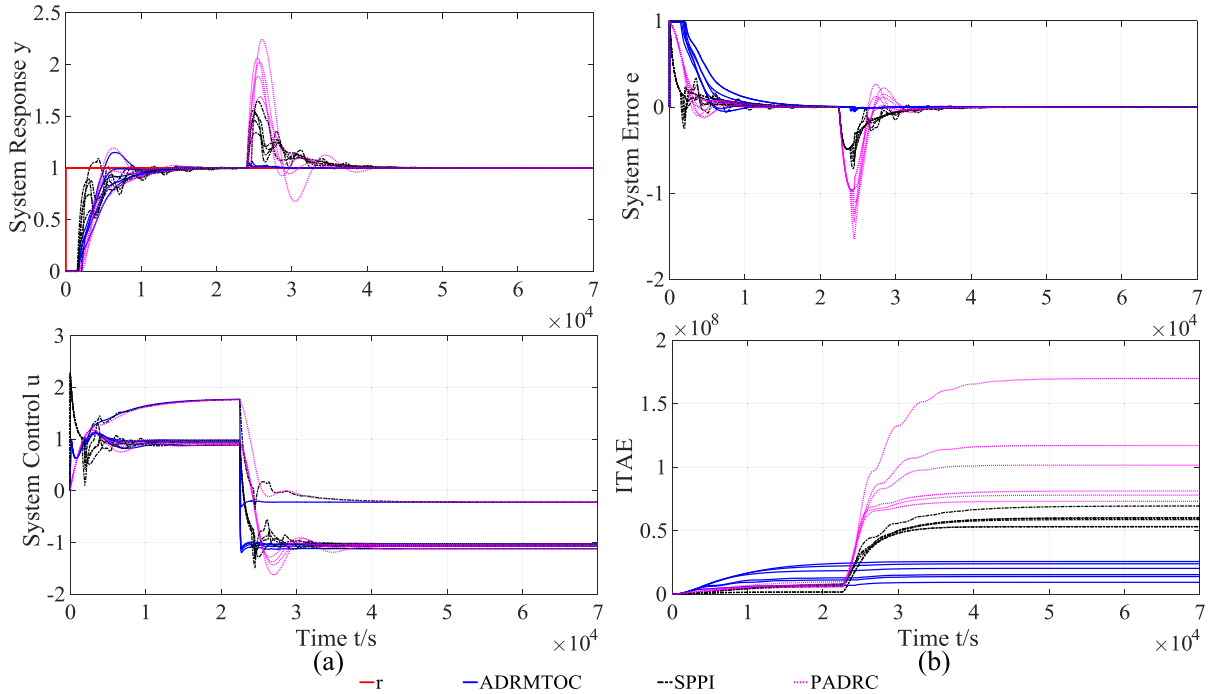| Performance index	Controller	SPPI	PADRC	ADRMTOC
Rapidity	Maximum deviation	0	0	0
	Adjustment time ($\times 10^3$)	6.4	6.4	6.4
	The value of ITAE ($\times 10^6$)	3.3728	3.238	8.9528
Robustness	$E_{dm}\%$	0.4721	0.93	0.0447
	Adjustment time ($\times 10^3$)	1.0	0.30	0
	The value of ITAE ($\times 10^7$)	5.5201	8.3644	1.0718

FIGURE 9. Experimental results of ADRMTOC, SPPI and PADRC results of six random parameters under non-ideal conditions.
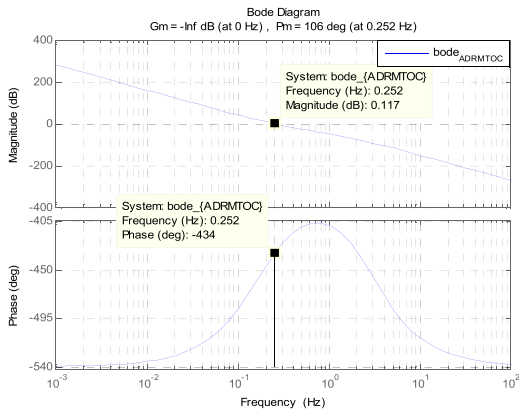

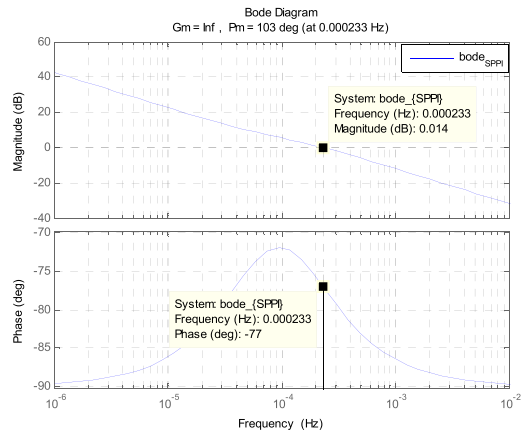**FIGURE 10.** Open-loop gain Bode diagram of ADRMTOC.

FIGURE 11. Open-loop gain Bode diagram of SPPI.

FIGURE 9(a) is the output response and control input of the system, FIGURE 9(b) is the error response of the system and ITAE; at the same time, the red line is the system set value curve, the blue line is the result curve of ADRMTOC, the black line is the result curve of SPPI, and the powder line is the result curve of PADRC.

It can be seen from FIGURE 9 that ADRMETOC has a stronger ability to suppress interference than SPPI and ADRC when the parameters are perturbed within a certain range. Also, the control curve is smoother and more concentrated than SPPI and ADRC. The error perturbation and ITAE value of ADRMTOC are smaller than those of SPPI and PADRC when the external interference signal exists. And the system under the control of PADRC will vibrate and cause harm to the system when the parameters stays in a certain range of

random perturbation. All these show that the performance index of ADRMTOC system is better than that of SPPI and PADRC.

B. FREQUENCY DOMAIN ANALYSIS OF ADRMTOC
In order to further analyze the robustness of ADRMTOC, the classical frequency domain analysis method is used to evaluate the system performance, and SPPI and PADRC are used as the comparison control algorithm. The open-loop gain Bode diagrams of ADRMTOC, SPPI and PADRC are shown in FIGURE 10 - 12, and the stable margins are calculated as shown in TABLE 6.

From FIGURE 10 - 12 and TABLE 6, the ADRMTOC has a much higher cross frequency than SPPI and PADRC,
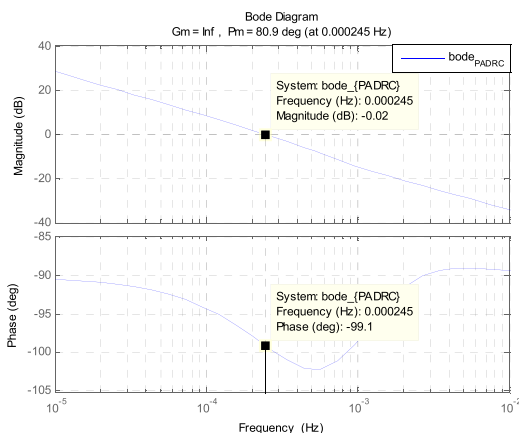
FIGURE 12. Open-loop gain Bode diagram of PADRC.

TABLE 6. Stable margin of three control algorithms.

Controller	Cross frequency (rad/s)	Phase margin (deg)
ADRMTOC	1.5822	106.2454
PADRC	0.0015	80.9337
SPPI	0.00146	103

which proves that the ADRMTOC can greatly improve the system's tracking speed than the other two control systems. Moreover, the phase margin of the ADRMTOC system is also larger than that of the SPPI and PADRC. The sensitivity of the system under the control of ADRMTOC is smaller and the delay perturbation is wider.

V. CONCLUSION

In this manuscript, ADRMTOC is designed to control the time-delay process by combining ADRC and MTOC, and its algorithm is compared with that of PADRC and SPPI. The simulation results show that, under ideal conditions, ADRM-TOC is slower than PADRC and SPPI when the response starts. However, in practical industries (under non-ideal models), the parameters of the prediction transfer function are difficult to be consistent with the actual function. When the model has a certain prediction quantity, the control effect of ADRMTOC is better than that of PADRC and SPPI. This is because the ADRMTOC algorithm compensates the time-delay factor more thoroughly. The control algorithm transforms the infinite-dimensional time-delay system into a finite-dimensional Non-time-delay system, overcomes the problem of asynchronization of input and output signals, and achieves real-time feedback control. When the system is disturbed by external information, the system can actively compensate and control, thus improving the robustness of the system. More significantly, the system curve of ADRMTOC is much smoother than that of PADRC and SPPI in the initial stage of response when the model parameters stays a certain range of perturbation. At this time, the system needs less control, saves industrial raw materials and brings considerable economic benefits. In any case, the interference suppression capability of ADRMTOC is far greater than that of PADRC and SPPI, and the disturbance recovery time is shorter than that of PADRC and SPPI. The theoretical analysis, parameter setting principle and simulation results of this manuscript are helpful to the application of ADRMTOC in time delay system. It provides not only a feasible method for the control of large time delay system, but also a better control scheme for the suppression of the strong interference signal of the system. Furthermore, in future research, attempts should be made to improve the ADRMTOC algorithm to improve its performance in the initial phase of response.

REFERENCES

[1] R. Langerak and J.W. Polderman , "Tools for stability of switching linear systems: Gain automata and delay compensation," in *Proc. Eur. Control Conf. CDC-ECC IEEE Conf. Decis. Control*, Dec. 2016, pp. 4867–4872.

[2] C. Tan, H. Zhang, and W. S. Wong, "Delay-dependent algebraic Riccati equation to stabilization of networked control systems: Continuous-time case," *IEEE Trans. Cybern.*, vol. 48, no. 10, pp. 2783–2794, Oct. 2017.

[3] G. L. Raja and A. Ali, "Smith predictor based parallel cascade control strategy for unstable and integrating processes with large time delay," *J. Process Control*, vol. 52, pp. 57–65, Apr. 2017.

[4] A. M. De Paor, "A modified Smith predictor and controller for unstable processes with time delay," *Int. J. Control*, vol. 41, no. 4, pp. 1025–1036, 1985.

[5] S.-I. Niculescu and A. M. Annaswamy, "An adaptive Smith-controller for time-delay systems with relative degree n* ≤2," *Syst. Control Lett.*, vol. 49, no. 5, pp. 347–358, 2003.

[6] W. Zhang, Y. Sun, and X. Xu, "Two degree-of-freedom Smith predictor for processes with time delay," *Automatica*, vol. 34, no. 10, pp. 1279–1282, 1998.

[7] I. Kaya, "IMC based automatic tuning method for PID controllers in a Smith predictor configuration," *Comput. Chem. Eng.*, vol. 28, no. 3, pp. 281–290, 2004.

[8] H. Khodadadi and A. Dehghani, "Fuzzy logic self-tuning PID controller design based on Smith predictor for heating system," in *Proc. 16th Int. Conf. Control, Autom. Syst.*, Oct. 2016, pp. 161–166.

[9] D. Ma and J. Chen, "Delay margin of low-order systems achievable by PID controllers," *IEEE Trans. Autom. Control*, vol. 64, no. 5, pp. 1958–1973, May 2018.

[10] S. Srivastava and V. S. Pandit, "A PI/PID controller for time delay systems with desired closed loop time response and guaranteed gain and phase margins," *J. Process Control*, vol. 37, pp. 70–77, Jan. 2016.

[11] Q. Jin, X. Du, and B. Jiang, "Novel centralized IMC-PID controller design for multivariable processes with multiple time delays," *Ind. Eng. Chem. Res.*, vol. 56, no. 15, pp. 4431–4445, 2017.

[12] R. Sumathi and P. Umasankar, "Optimal design of fractional order PID controller for time-delay systems: An IWLQR technique," *Int. J. Gen. Syst.*, vol. 47, no. 1, pp. 714–730, 2018.

[13] K. K. Tan, S. Zhao, and J. X. Xu, "Online automatic tuning of a proportional integral derivative controller based on an iterative learning control approach," *IET Control Theory Appl.*, vol. 1, no. 1, pp. 90–96, Jan. 2007.

[14] H. Wang, J. Liu, and Y. Zhang, "New results on eigenvalue distribution and controller design for time delay systems," *IEEE Trans. Autom. Control*, vol. 62, no. 6, pp. 2886–2901, Jun. 2017.

[15] H. Li, J. Wang, L. Wu, H.-K. Lam, and Y. Gao, "Optimal guaranteed cost sliding-mode control of interval type-2 fuzzy time-delay systems," *IEEE Trans. Fuzzy Syst.*, vol. 26, no. 1, pp. 246–257, Feb. 2018.

[16] X. Su, P. Shi, L. Wu, and M. V. Basin, "Reliable filtering with strict dissipativity for T-S fuzzy time-delay systems," *IEEE Trans. Cybern.*, vol. 44, no. 12, pp. 2470–2483, Dec. 2014.

[17] J. Yi, J. Li, and J. Li, "Adaptive fuzzy output feedback control for nonlinear nonstrict-feedback time-delay systems with full state constraints," *Int. J. Fuzzy Syst.*, vol. 20, no. 6, pp. 1730–1744, Aug. 2018.

[18] S. Vrkalovic, E.-C. Lunca, and I.-D. Borlea, "Model-free sliding mode and fuzzy controllers for reverse osmosis desalination plant," *Int. J. Artif. Intell.*, vol. 16, no. 2, pp. 208–222, 2018.

[19] L. Wang and H.-K. Lam, "A new approach to stability and stabilization analysis for continuous-time Takagi–Sugeno fuzzy systems with time delay," *IEEE Trans. Fuzzy Syst.*, vol. 26, no. 4, pp. 2460–2465, Aug. 2018.

[20] X. Li and K. Merhan, "Model-based control and stability analysis of discrete-time polynomial fuzzy systems with time delay and positivity constraints," *IEEE Trans. Fuzzy Syst.*, to be published. doi: 10.1109/TFUZZ.2019.2893344.

[21] J. Liu, Z.-G. Wu, D. Yue, and J. H. Park, "Stabilization of networked control systems with hybrid-driven mechanism and probabilistic cyber attacks," *IEEE Trans. Syst., Man, Cybern., Syst.*, to be published. doi: 10.1109/TSMC.2018.2888633.

[22] H. Ma, Y. Zhang, and G. Tang, "Optimized BP neural network state feedback control with time delay for offshore platforms under wave forces," in *Proc. 4th Int. Conf. Inf., Comput. Social Syst. (ICCSS)*, 2017, pp. 517–522.

[23] F. Pazhooh, F. Shahraki, J. Sadeghi, and M. Fakhroleslam, "Multivariable adaptive neural network predictive control in the presence of measurement time-delay; application in control of Vinyl Acetate monomer process," *J. Process Control*, vol. 66, pp. 39–50, Jun. 2018.

[24] H. Wang, P. X. Liu, and S. Liu, "Adaptive neural synchronization control for bilateral teleoperation systems with time delay and backlash-like hysteresis," *IEEE Trans. Cybern.*, vol. 47, no. 10, pp. 3018–3026, Oct. 2017.

[25] T. Q. Dinh, K. K. Ahn, and J. Marco, "A novel robust predictive control system over imperfect networks," *IEEE Trans. Ind. Electron.*, vol. 64, no. 2, pp. 1751–1761, Feb. 2017.

[26] A. Sargolzaei, K. K. Yen, M. N. Abdelghani, S. Sargolzaei, and B. Carbunar, "Resilient design of networked control systems under time delay switch attacks, application in smart grid," *IEEE Access*, vol. 5, pp. 15901–15912, 2017.

[27] Q. Yan, J. Cai, L. Wu, and Q. Zhou, "Error-tracking iterative learning control for nonlinearly parametric time-delay systems with initial state errors," *IEEE Access*, vol. 6, pp. 12167–12174, Jan. 2018.

[28] H. F. Tao, W. Paszke, E. Rogers, H. Z. Yang, and K. Galkowski, "Iterative learning fault-tolerant control for differential time-delay batch processes in finite frequency domains," *J. Process Control*, vol. 56, pp. 112–128, Aug. 2017.

[29] S. Preitl, R.-E. Precup, Z. Preitl, S. Vaivoda, S. Kilyeni, and J. K. Tar, "Iterative feedback and learning control. Servo systems applications," *IFAC Proc. Volumes*, vol. 40, no. 8, pp. 16–27, 2007.

[30] G. Xiang, Y. Yang, and Q. Yang, "Twice optimal control for a kind of first order system with dead-time," (In Chinese), *Inf. Control*, vol. 24, no. 4, pp. 208–214, 1995.

[31] Q. Yang, Y. Yang, and G. Xiang, "ITAE twice optimal control for a kind of two-capacity system with time-delay," (In Chinese), in *Proc. Chin. Control Conf.*, 1995, pp. 475–480.

[32] H. Zhang, Q. Wang, and G. Xiang, "Nonlinearized design for twice-optimal control of a second-order dead-time system," (In Chinese), *Inf. Control*, vol. 46, no. 6, pp. 664–670, 2017.

[33] G. Xiang, *Time-delay System 0ptimization Control*. Beijing, China: China Electric Power Press, (In Chinese), 2009.

[34] B. Ban, Q. Wang, and G. Xiang, "Construction pruning for twice optimal control of pure integrating process with long time delay," in *Proc. 27th Chin. Control Decis. Conf.*, 2015, pp. 2782–2788.

[35] X. Wang, W. Li, W. Wei, and M. Zuo, "Active disturbance rejection twice optimal control for time delay system," in *Proc. Chin. Intell. Syst. Conf.*, 2017, pp. 731–737.

[36] J. Q. Han, "Auto-disturbances rejection controller and it's applications," (In Chinese), *Control Decis.*, vol. 13, no. 1, pp. 19–23, 1998.

[37] A. Benrabah, D. Xu, and Z. Gao, "Active disturbance rejection control of *LCL*-filtered grid-connected inverter using Padé approximation," *IEEE Trans. Ind. Appl.*, vol. 54, no. 6, pp. 6179–6189, Nov./Dec. 2018.

[38] Y. Xia, M. Fu, C. Li, F. Pu, and Y. Xu, "Active disturbance rejection control for active suspension system of tracked vehicles with gun," *IEEE Trans. Ind. Electron.*, vol. 65, no. 5, pp. 4051–4060, May 2018.

[39] J. Q. Han, "A class of extended state observers for uncertain systems," (In Chinese), *Control Decis.*, vol. 10, no. 1, pp. 85–88, 1995.

[40] C. Wang, Z. Zuo, Z. Qi, and Z. Ding, "Predictor-based extended-state-observer design for consensus of MASs with delays and disturbances," *IEEE Trans. Cybern.*, vol. 49, no. 4, pp. 1259–1269, Apr. 2018.

[41] R.-C. Roman, R.-E. Precup, E. M. Petriu, and F. Dragan, "Combination of data-driven active disturbance rejection and Takagi–Sugeno fuzzy control with experimental validation on tower crane systems," *Energies*, vol. 12, no. 8, pp. 1–19, 2019.

[42] D. Tang, Z. Gao, and X. Zhang, "Design of predictive active disturbance rejection controller for turbidity," (In Chinese), *Control Theory Appl.*, vol. 34, no. 1, pp. 101–108, 2017.

● ● ●